Korean J. Chem. Eng., 34(3), 797-805 (2017)
DOI: 10.1007/s11814-016-0333-x

pISSN: 0256-1115
eISSN: 1975-7220

Comparison of metabolite profiling of *Ralstonia eutropha* H16 *phaBCA* mutants grown on different carbon sources

Dae-Kyun Im[*,‡], Seok Hun Yun[,***,‡], Joon-Young Jung[**], Jinwon Lee[***,†], and Min-Kyu Oh[*,†]**

*Department of Chemical and Biological Engineering, Korea University, Seoul 02841, Korea
**CJ Research Institute of Biotechnology, Suwon 16495, Korea
***Department of Chemical and Biomolecular Engineering, Sogang University, Seoul 04107, Korea
(*Received 24 October 2016 • accepted 20 November 2016*)

Abstract−Metabolite profiling was conducted to monitor the metabolic differences of the *Ralstonia eutropha* H16, polyhydroxybutyrate (PHB) producing strain, when grown on different sole carbon sources and to identify the effect of the deletion of the PHB production pathway. The combination of rapid filtration and boiling ethanol extraction successfully extracted intracellular metabolites. Accumulation of acetyl-CoA was detected when the strain was grown on fructose. Whereas, lower adenylate energy charge (AEC) ratio and cell mass was identified on the cells grown on acetate. No significant difference was detected between the wild type and mutant strain except metabolites in the PHB synthetic pathway. Increased PHB production is expected on fructose due to the accumulation of AcCoA, while it is more difficult to improve the production on acetate because of lower metabolic precursor level and AEC ratio.

Keywords: *Ralstonia eutropha* H16, PHA, Metabolite Profiling, GC-EI-MS, LC/TOF/MS, Adenylate Energy Charge (AEC) Ratio

INTRODUCTION

Polyhydroxyalknoates (PHAs) are produced by more than 300 species of bacteria as an intracellular carbon and energy storage material [1]. Due to their physical properties and biodegradability, PHAs can be used as alternatives to plastics [2,3]. *Ralstonia eutropha* H16, a gram negative bacterium, is well known to be a PHA producing bacterium, as this strain can produce poly[*(R)*-3-hydroxybutyrate] [P(3HB)] efficiently from fructose, gluconate, fatty acids and vegetable oils with cellular content up to 60-80 wt% [4]. In the pathway to P(3HB), two molecules of acetyl-CoA are condensed to acetoacetyl-CoA by acetyl-CoA acetyltransferase (PhaA), which is subsequently reduced to *(R)*-3-hydroxybutyryl (3HB)-CoA by NADPH dependent acetoacetyl-CoA reductase (PhaB). Lastly, the resultant 3HB-CoA are polymerized to P(3HB) by PHA polymerase (PhaC) [5,6].

The improvement of P(3HB) production has progressed via molecular and fermentation strategies [7]. For example, inactivation of pyruvate carboxylase or the alginate synthesis pathway improved the specific production of P(3HB) several times compared with the wild type strain [8]. The modification of regulatory systems was also used to improve PHA synthesis. For example, the expression of the P(3HB) biosynthetic operon was negatively regulated by nitrogen related phosphotransferase (PTS^{Ntr}) [9]. Therefore, inactivation of this regulatory protein (PtsN) increased the specific production of P(3HB) by 77% [10]. Finding new alternative carbon sources is one of the key aspects of fermentation strategies, hence several candidates, such as waste glycerol, corn syrup, cane molasses, palm oil, acetate and pretreated lignocellulosic biomass, have been used for P(3HB) production [11-13]. To date, the most widely studied strain for P(3HB) production is the *R. eutropha* species [9].

Metabolome analysis involves comprehensive identification and quantification of intracellular metabolites. Mass spectrometry (MS) based metabolome studies have been performed to understand the relationship between cell phenotype and cellular metabolic status [14, 15]. Despite the many advantages of metabolomics study in biochemical production, the experimental procedure, such as the choice of quenching and metabolite extraction, is still difficult and should be optimized depending on target metabolites or host strains [16-18]. So far, metabolome analysis of *R. eutropha* species has been very limited [4].

The purpose of this study was the comparative metabolite profiling analysis of central carbon metabolism on different carbon sources and the effect of inactivating the P(3HB) synthesis pathway. For this purpose, the *R. eutropha* H16 wild type strain and the deletion mutant of P(3HB) synthesis genes (PhaA, PhaB and PhaC) were cultivated on fructose and acetate. Four sample preparation methods were evaluated to optimize sample preparation for the *R. eutropha* H16 strains. The results indicated distinct profiles for the intracellular metabolite levels under different carbon sources, including in CoA thioesters in addition to ATP availability.

EXPERIMENTAL SECTION

1. Materials

The defined growth medium contained (per liter medium) 3.6 g

†To whom correspondence should be addressed.
E-mail: mkoh@korea.ac.kr, jinwonlee@sogang.ac.kr
‡Both authors contributed equally to this manuscript.
‡This article is dedicated to Prof. Ki-Pung Yoo on the occasion of his retirement from Sogang University.

NaH_2PO_4, 2.84 g Na_2HPO_4, and 1 ml trace elements (0.5 g $CuSO_4 \cdot 5H_2O$, 2.4 g $ZnSO_4 \cdot 7H_2O$, 2.4 g $MnSO_4 \cdot H_2O$, and 15 g $FeSO_4 \cdot 7H_2O$ per liter). Carbon (fructose (10 g/L) or sodium acetate (6 g/L)) and nitrogen (NH_4Cl) sources were added as indicated. Gentamicin (50 μg mL^{-1}) was added for the selection of mutants. All the chemicals and metabolite standards for GC-EI-MS and LC/TOF/MS were purchased from Sigma Aldrich (Sigma-Aldrich, St. Louis, MO, USA).

2. Strain and Growth Conditions

R. eutropha H16 ATCC17699 and its *phaCAB* mutant, RHM5 [19] were precultured in TSB medium (Sigma-Aldrich, St. Louis, MO, USA) for 24 h at 30 °C with shaking at 250 rpm. Then, the cells were harvested by centrifugation (13,500 rpm, 10 min), washed twice with distilled water, and transferred to 50 mL defined growth media with the initial OD_{600} at 0.05 followed by incubation with shaking at 250 rpm. 5 mL of the cell broth was taken at 24 h on fructose (10 g/L) and at 48 h on acetate (6 g/L) at the mid-exponential growth phase for metabolite profiling.

3. Sampling Preparation Methods for Intracellular Metabolites

For the cold methanol quenching method, 3 mL of cell broth was injected into 9 mL of −40 °C methanol/water solution (75% v/v) and centrifuged for 10 min at 15,000 rpm. Then, the supernatant was removed and the extraction solution was added. For the fast filtration method, 5 mL of the cell broth was filtered with a 0.20 μm membrane disk filter (Merck-Millipore, German) attached to a filtering apparatus with a vacuum pump and washed with 20 mL of 4 °C PBS buffer. Then, the disk filter with the sample was immersed into a 50 mL conical tube containing ice-cold extraction solution and the conical tube was immediately immersed into liquid nitrogen.

For boiling ethanol extraction, 4 mL of 75% (v/v) ethanol/water hot extraction solution was added to the sample and incubated at 90 °C for 5 min. Afterward, the samples were cooled to 4 °C and centrifuged at 12,000 rpm for 10 min. The supernatants (1.5 mL) were transferred to a fresh conical tube and 10 μL of 280 μmol L^{-1} erythritol was added as an internal standard, followed by vaporization by speed vacuum (Hanil, Korea). For chloroform/methanol extraction, 3 mL of chloroform/methanol (1 : 1 v/v) extraction solution was added and the samples were vortexed for 2 min, followed by the addition of 1 mL deionized water. The samples were cooled and centrifuged and 500 μL of the upper water phase was transferred to a fresh conical tube with 10 μL of internal standard, followed by vaporization. The samples were stored at −80 °C in a deep freezer until analyzed.

The extracted metabolites underwent two-stage chemical derivatization for GC-EI-MS analysis. Briefly, 50 μL of 2 wt% hydroxylamine hydrochloride in pyridine was added to the sample and the mixture was heated at 70 °C for 50 min. After cooling, 80 μL of N-Methyl-N-(trimethylsilyl)trifluoroacetamide with 1 vt% trimethylchlorosilane (Sigma-Aldrich) was added to the mixture and heated at 70 °C for 50 min.

4. GC-EI-MS Analysis Condition

Derivatized intracellular metabolite samples were analyzed using a Bruker 450-GC instrument coupled with the Bruker 300-MS single quadruple mass spectrometer (Bruker Inc. Fremont, USA). The system utilized the silica capillary column BR-5ms (5% Diphenyl/95% Dimethyl poly siloxane, 30 m×0.25 mm ID, 0.25 μm df, Bruker Inc, Fremont, USA). Helium gas (99.999% purity) was used as a carrier gas with 1.5 mL min^{-1} of gas flow rate. Column oven temperature was initially kept at 70 °C for 1 min, increased to 80 °C at a rate of 2 °C min^{-1} and held for 1 min, increased to 200 °C at a rate of 6 °C min^{-1} and held for 3 min, then increased to 270 °C at a rate of 15 °C min^{-1} where it was held for 5 min. The temperatures for the front inlet, transfer line, and ion source were 270, 270, and 200 °C, respectively. The injected volume for each sample was 1 μL in 1 : 15 split ratio mode. The mass spectrometry data were acquired in full scan mode with the m/z range of 50-800 for metabolite identification and single ion monitoring (SIM) mode for relative metabolite quantification after a solvent delay of 7 min. The metabolite intensity for each sample was normalized by the internal standard intensity.

5. LC/TOF/MS Analysis Condition

Intracellular metabolites were also analyzed by UPLC Q-TOF MS (Waters Corporation, Milford, MA, United States). 5 μL samples were injected and metabolites were separated using an ion pairing-reverse phase method for UPLC systems [20]. The Waters Acquity UPLC® HSS T3 end-capped reverse phase column (150 mm×2.1 mm×1.8 μm) was used with a column temperature of 35 °C. Gradient mobile phases A (10 mmol L^{-1} tributylamine and 15 mmol L^{-1} acetic acid in distilled water) and B (100% methanol) were used and the flow rate was 0.3 mL min^{-1} (Table S1). Selective detection of compounds was achieved by coupling the liquid chromatograph to Waters Xevo QTOF MS (Waters Corporation, Milford, MA, United States). The source temperature was set to 100 °C with a cone gas flow of 30 L h^{-1}, and the desolvation gas temperature and flow rate were set to 45 °C and 500 L h^{-1}, respectively. The capillary voltage was set to 2.5 kV and the cone voltage was set to 20 V. Centroid data were collected from m/z 50 to 1,000 with a scan time of 0.3 s. Leucine-enkephalin was used as the lock mass (m/z 554.2615 in negative mode). Both acquisition and peak integration were performed with Masslynx software version 4.1 (Waters Corporation, Milford, MA, United States).

6. Determination of Extracellular Metabolites

Extracellular metabolites such as fructose and acetate were analyzed by high-performance liquid chromatography using an ACME-9000 (Young-Lin instrument, Seoul, Korea) equipped with an SH1011 column (Shodex, Tokyo, Japan). The mobile phase used was 2.5 mmol L^{-1} H_2SO_4 with a flow rate of 0.5 mL min^{-1}.

Amino acids were analyzed by using the HITACHI AAA L-8900 system (Hitachi High-Technologies Corporation, Nishi-Shimbashi, Tokyo, Japan). The injection volume was 10 μL with full loop injection, and a ninhydrin reaction was performed for amino acid analysis as previously described [21]. The Hitachi Reaction column (Hitachi High-Technologies Corporation, Nishi-Shimbashi, Tokyo, Japan) was used for the ninhydrin reaction at 135 °C and an Ion Exchange #2622 PH Column with dimensions of 7.8 mm×150 mm (Hitachi High-Technologies Corporation, Nishi-Shimbashi, Tokyo, Japan) was used for separation at 57 °C. Four pH gradient buffers (pH 1-4) and a stabilizing solution (RG) were used as the mobile phase A and the flow rate was 0.40 ml/min. Ninhydrin solution was used as phase B and the flow rate was 0.35 ml/min. The mobile phase gradients are described in detail in Table S1.

7. PHB Quantification

After the cells were cultured for 96 h, 40 mL of culture broth was centrifuged at 15,000 rpm for 10 min. After washing with 20 mL of

distilled water, the cell pellets were stored in a dry oven overnight. The dried cell pellets were dispersed with 11 mL of chloroform mixed with 4 mL of a sodium hypochlorite solution (30% v/v). After incubation at 37 °C overnight, the samples were centrifuged at 15,000 rpm for 10 min at 30 °C. Three distinct phases were formed after the centrifugation. 5 mL of the chloroform phase at the bottom was carefully collected and the PHB was recovered by non-solvent (80% v/v methanol) precipitation [22].

Table 1. Measured metabolite concentration depending on sampling methods by GC-EI-MS (unit: measured metabolite intensity/measured internal standard intensity)

Cell prep. method	Cold methanol	Cold methanol	Rapid filtration	Rapid filtration
Extraction method	M : C : W*	Boiling ethanol	M : C : W*	Boiling ethanol
Pyr	0.318±0.120	0.114±0.043	ND	1.099±0.390
Ala	0.186±0.067	0.067±0.024	0.088±0.059	2.308±0.878
Val	0.234±0.000	0.084±0	0.154±0.042	0.610±0.391
Leu	0.354±0.197	0.127±0.071	0.059±0.032	0.348±0.269
Ile	0.105±0.052	0.038±0.019	0.132±0.050	0.276±0.166
Gly	0.162±0.000	0.058±0	0.220±0.128	0.458±0.206
Suc	0.207±0.045	0.074±0.016	1.501±0.674	0.271±0.072
Fum	0.135±0.031	0.048±0.011	1.121±0.267	0.252±0.078
Ser	2.165±0.411	0.774±0.147	6.610±3.433	6.015±2.865
Thr	2.953±0.478	1.055±0.171	3.336±1.806	4.825±2.134
Mal	ND	ND	0.656±0.249	0.143±0.055
Met	0.033±0.041	0.012±0.015	0.020±0.008	0.081±0.022
Asp	0.114±0.104	0.041±0.037	2.286±2.340	0.688±0.174
aKG	ND	ND	ND	1.903±0.790
Glu/Gln	17.345±3.944	6.196±1.409	147.211±100.437	57.752±23.601
Phe	0.189±0.000	0.068±0	0.160±0.110	0.185±0.086
Asn	ND	ND	1.146±0.161	0.086±0.018
2PG	ND	ND	0.987±0.883	0.149±0.070
3PG	0.090±0.031	0.032±0.011	1.920±0.832	1.403±0.358
Cit	0.865±0.733	0.309±0.262	0.314±0.115	0.300±0.077
Lys	0.579±0.306	0.207±0.110	1.543±0.920	1.249±0.530
Tyr	0.036±0.000	0.013±0	0.200±0.094	0.136±0.050
R5P	ND	ND	ND	0.095±0.029
F6P	2.886±0.473	1.031±0.169	0.568±0.327	0.418±0.112
G6P	0.883±0.421	0.316±0.151	0.344±0.246	0.331±0.084
6PG	2.102±0.738	0.751±0.264	0.523±0.401	0.739±0.233

*M : C : W stands for methanol:chloroform:water extraction method
Analysis was performed, biological triplicates and technical duplicates (n=6)

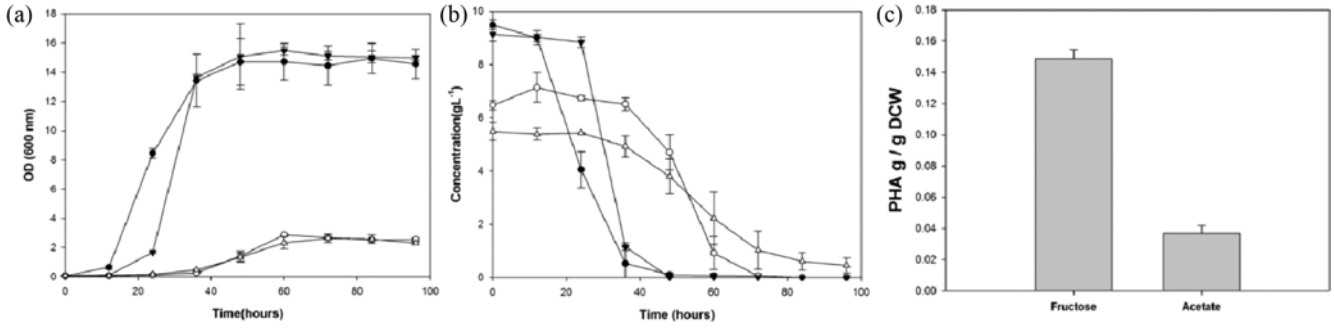

Fig. 1. Time profiles of *Ralstonia eutropha* H16 strain on two different carbon sources and PHAs production per dry cell weight. (a) and (b) growth pattern and carbon consumption pattern of *Ralstonia eutropha* H16 wild type strain on fructose (●) and acetate (○) condition, RHM5 on fructose (▼) and acetate (△) respectively. (c) Polyhydroxyalknoates (PHAs) production per dry cell weight on fructose and acetate condition.

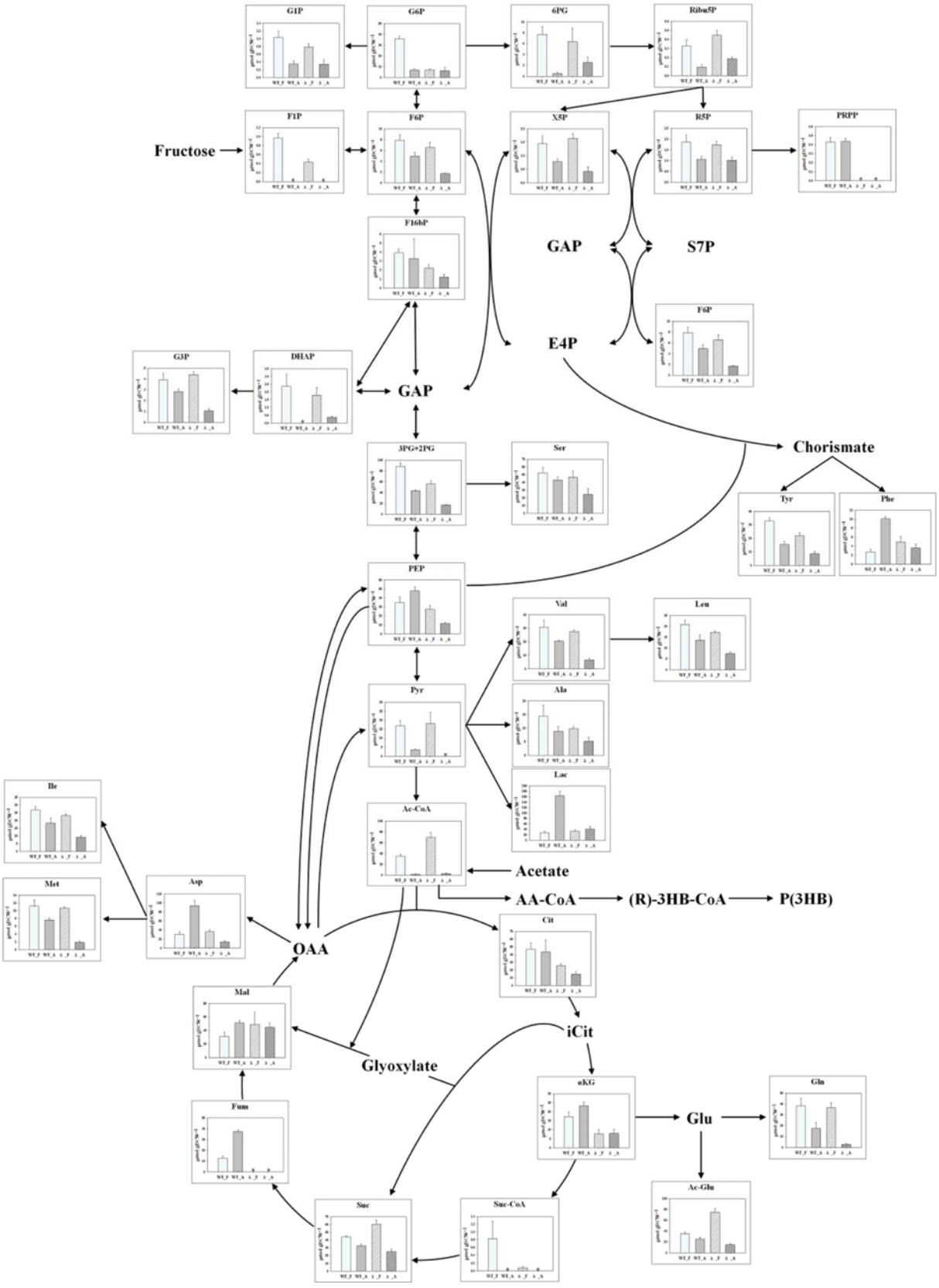

Fig. 2. Metabolite profiles of *Ralstonia eutropha* H16 wild type and PHA production genes deleted strains on fructose and acetate, respectively. White bar denotes *Ralstonia eutropha* H16 wild type strain grown on fructose, grey bar denotes grown on acetate, respectively. White and diagonal lined bar denotes PHA production genes deleted strain grown on fructose, grey and diagonal lined bar denotes grown on acetate, respectively. Analysis was performed, biological triplicates and technical duplicates (n=6).

RESULTS

1. Optimization of Sample Preparation

Sample preparation steps, which consisted of quenching the intracellular metabolites and extracting the metabolites, were optimized for proper quantification of metabolites. Two different quenching methods, cold methanol and fast filtration, were combined with two extraction methods, boiling ethanol and methanol-chloroform-water. Therefore, four different methods were tested with *R. eutropha* H16 cultured with fructose. Each sampling method was conducted according to previously described methods [17,23-26] with minor modifications.

The cold methanol quenching method did not provide proper identification of peaks during GC-EI-MS analysis, resulting in inconsistent quantification results (Table 1). It has been reported that during cold methanol quenching, metabolite leakage can be severe, resulting in low and inconsistent metabolite concentrations after the experiment [27-29]. Indeed, some metabolic intermediates, such as malic acid, 2-oxoglutarate, and ribose-5-phosphate, were not detected in cold methanol quenching samples, but they were successfully detected with the fast filtration method. Although the fast filtration method requires more time to harvest and wash the cells compared to cold methanol quenching [30], it provides more reliable results, such as in metabolite identification and the consistency of metabolite concentrations, as reported in metabolomics study with other bacteria [31,32]. Between boiling ethanol and methanol-chloroform-water extraction methods, boiling ethanol provided more consistent results with GC-EI-MS (Table 1) despite concerns over the stability of the metabolites at high temperature. Therefore, combination of fast filtration and boiling ethanol was chosen as the sample preparation method in this experiment.

When the prepared sample was derivatized and applied to GC-EI-MS, roughly 47 metabolites were quantified, which included many central carbon metabolites of *R. eutropha* H16 (Table 1). However, despite the many advantages of GC-EI-MS, several key metabolites of the strain, such as F16bP, G1P, F1P, and CoA derivatives, such as Ac-CoA, AA-CoA and 3HB-CoA, were not detected. Therefore, LC/MS/MS was used as the primary tool for monitoring and quantifying those metabolites. When the samples were taken from *R. eutropha* H16 on fructose, prepared without derivatization and analyzed by LC/TOF/MS, all the metabolites in Table 1 were successfully identified (data not shown). In addition, many important metabolites for characterizing the phenotype of the *R. eutropha* H16, such as adenosine phosphate and CoA derivatives, were quantified successfully in LC/TOF/MS, but not in GC-EI-MS. The concentrations detected by LC/TOF/MS were reasonably correlated with those detected by GC-EI-MS (Fig. S1).

2. Metabolites of *R. eutropha* Grown with Fructose or Acetate as a Sole Carbon Source

We cultivated *R. eutropha* H16 on fructose and acetate and detected the metabolites in each condition to identify the differences in metabolism. Their phenotypic differences, such as the growth curve, carbon source consumption rate, specific production of PHB and amino acid secretion to media, are shown in Fig. 1 and Table S2. The growth rate (g DCW h^{-1}), carbon consumption rate (g h^{-1}) and PHB production amount (g PHB g DCW^{-1}) were 6.78, 2.73,

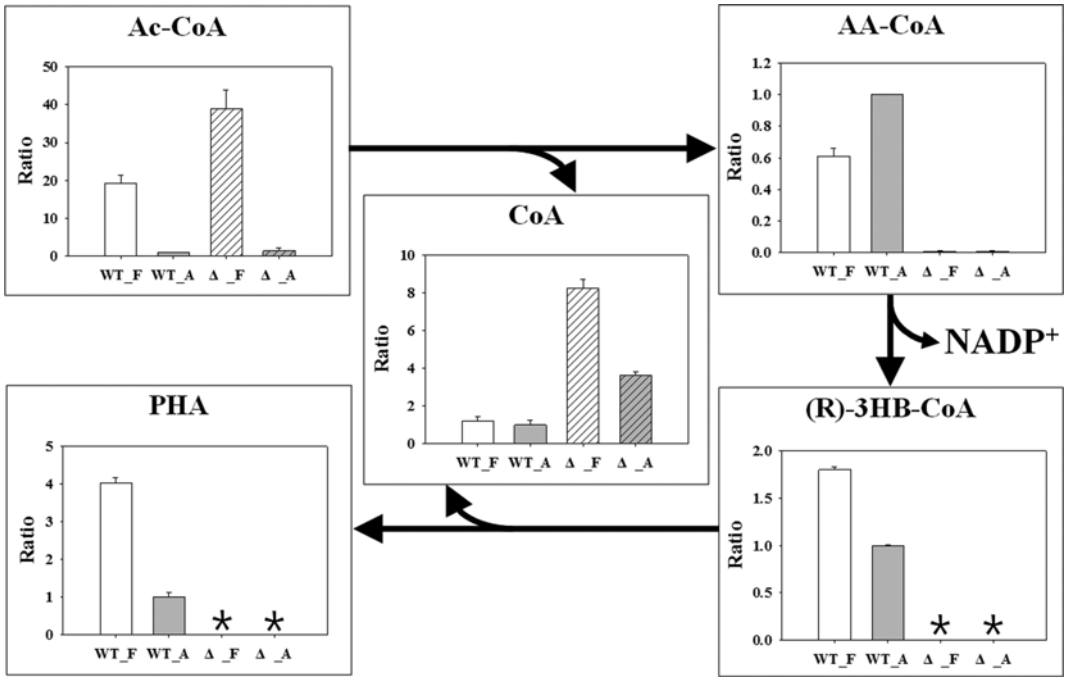

Fig. 3. Metabolite profiles of PHAs synthetic pathway related metabolite in *Ralstonia eutropha* H16 wild type and PHAs synthetic genes deleted strains on fructose and acetate. White bar denotes *Ralstonia eutropha* H16 wild type strain grown on fructose, grey bar denotes grown on acetate, respectively. White and diagonal lined bar denotes PHAs synthetic genes deleted strain grown on fructose, grey and diagonal lined bar denotes grown on acetate, respectively. Analysis was performed, biological triplicates and technical duplicates (n=6).

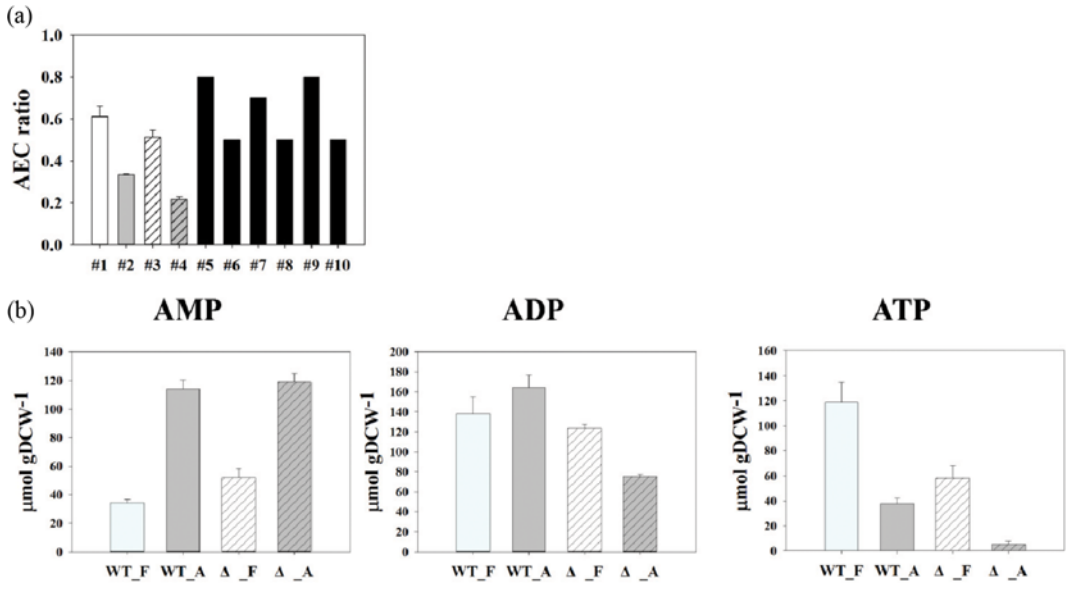

Fig. 4. Determination of adenosine mono-, di-, tri- phosphates and adenylate energy charge ratio for *Ralstonia eutropha* H16 wild type strain (solid) and PHAs synthetic genes deleted strain (diagonal pattern) on fructose (white bar) and acetate (grey bar), respectively. (a) Level of Adenosine mono-phosphate (AMP), adenosine di-phosphate (ADP) and Adenosine tri-phosphate (ATP) on fructose and acetate, respectively. (b) Calculated AEC ratio for each condition and reference values in several microbes (#1 WT on fructose, #2 WT on acetate, #3 PHAs synthetic genes deleted strain on fructose, #4 PHAs synthetic genes deleted strain on acetate, #5 *E. coli*: growth phase, #6 *E. coli*: stationary phase, #7 *B. subtilis*: growth phase, #8 *B. subtilis*: stationary phase, #9 *S. cerevisiae*: growth phase, #10 *S. cerevisiae*: stationary phase). Analysis was performed, biological triplicates and technical duplicates (n=6).

and 4.02 times higher on fructose than acetate, respectively, consistent with a previous study [33]. However, the specific carbon consumption rate (mmol g DCW^{-1} h^{-1}) was 3.94 times higher on acetate than fructose, suggesting a highly active carbon metabolism for energy supplementation on acetate.

The quantifications of sugar, sugar phosphate, carboxylic acids and amino acids in the central metabolism, along with intermediates in PHB synthesis within the *R. eutropha* H16 wild type strain were quantified with LC/TOF/MS, and the results are shown in Fig. 2 and 3. When the cells were cultivated on fructose, the pool sizes for the hexose-phosphate and pentose-phosphates were 1.8-5 times higher than those on acetate. Also, most of the amino acids derived from glycolysis and the PP pathway showed similar results as hexose- or pentose-phosphate. Especially, F1P, an intermediate of the fructose utilization pathway, was detected only on fructose medium, but not on acetate. Another significant difference was observed with Ac-CoA. The level of Ac-CoA was expected to be higher on acetate, because it is the first central metabolite when acetate is utilized [34]. However, the level was almost 20-fold higher on fructose than on acetate. Meanwhile, metabolites in or derived from the citric acid cycle showed very different patterns. Metabolite levels were almost similar on both carbon sources except for Suc-CoA and some important metabolites, Fum, Mal, Asp, and PEP showed higher concentrations on acetate.

We also monitored the metabolite concentrations of the strain with no PHB synthesis genes (*ΔphaABC*) under the same conditions [19]. Generally, the effect of gene deletion on metabolite concentrations was not as significant as that of the carbon source, except in the PHB synthetic pathway. Only a few metabolites, PRPP, Suc-CoA, AA-CoA, etc., showed significant reduction of their concentrations in the deletion mutant. Interestingly, free CoA concentration was much higher in the mutant than in the wild-type (Fig. 3). When the mutant was grown on fructose and acetate, the metabolite pattern was very similar to that of the wild type. For example, the concentrations of most metabolites were higher on fructose (Fig. 2).

3. Energy Charge Analysis

The adenylate energy charge (AEC) ratio for different carbon sources was calculated (Fig. 4). Compared with other species in the growth phase (*Eschericia coli*: 0.8, *Bacillus subtilis*: 0.7 and *Saccharomyces cerevisiae*: 0.8), the value of the AEC ratio in the *R. eutropha* H16 wild type strain was low on fructose (0.61) and even lower on acetate (0.33) (Fig. 4(a)). The relative level of ATP was 3.13 times lower on acetate than on fructose. In the deletion mutant for PHB synthetic genes, the value of the AEC ratio was slightly lower than that of the wild type, at 0.51 on fructose and 0.22 on acetate, respectively (Fig. 4(b)).

DISCUSSION

We optimized the experimental procedure and monitored the metabolite concentrations of the *R. eutropha* H16 wild type strain and the deletion mutant of PHB synthetic pathway genes. Based on the metabolite concentrations, a few interesting phenotypes could be confirmed. For example, the annotation information and biochemical analysis information suggested that phosphofructokinase and 6-phosphogluconate dehydrogenase homologs were absent from the *R. eutropha* H16 genome [33,34]. Even with no

annotated 6-phosphogluconate dehydrogenase, the presence of pentose 5 phosphates suggested that the non-oxidative PP pathway was active in supplying essential metabolites derived from pentose. Another interesting result is in regard to the gluconeogenesis pathway, which is known to be induced to produce five or six carbon metabolites when a carbon source like acetate is used as the sole carbon source. Because *R. eutropha* H16 does not contain phosphofrutokinase, which is an essential gene for the Embden-Meyerhof-Parnas pathway, F16bP could not be synthesized from glycolysis. However, F16bP was detected during the cultivation on fructose, suggesting that the gluconeogenesis pathway is activated in the hexose condition. Previous metabolite profile research was also consistent with this result [4].

Then *R. eutropha* H16 utilizes acetate, a non-fermentative carbon source, as the sole carbon source; the metabolite profiling pattern is similar to that with octanoate as the sole carbon source [4]. Intermediates of the citric acid cycle, PEP and Asp, which are directly derived from OAA on acetate through the glyoxylate shunt pathway, were higher than in the fructose condition. To synthesize metabolites like 3PG, hexose and pentose, the gluconeogenesis pathway is known to be active under the acetate condition in bacteria [35]. Abundant levels of PEP implied that phosphoenolpyruvate carboxykinase (pepck) was highly activated on acetate to supply carbon flux to the gluconeogenesis pathway from the citric acid cycle and the glyoxylate shunt pathway [36]. Unlike the octanoate condition, sugar phosphates and Ac-CoA levels were much lower on acetate than on fructose. Considering the high specific acetate uptake rate, we presumed that Ac-CoA may be converted to metabolites to supply carbon atoms for biosynthesis through the glyoxylate shunt pathway or for ATP synthesis through the TCA cycle. Interestingly, SUC-CoA was not detected in the acetate condition, which strongly supports the theory that the glyoxylate shunt pathway is a major pathway in the acetate condition.

The most drastic difference between the metabolite profiles for the two different carbon sources was the pathway from PYR to AA-CoA. Among the two, Ac-CoA showed the biggest difference, at 19.25 times higher on fructose. When the PHB production genes were deleted, the difference in Ac-CoA on fructose was even greater. Therefore, the high level of Ac-CoA may suggest that further improvements of PHB production can be achieved on fructose by increasing the carbon flux to PHB. Interestingly, AA-CoA was higher on acetate, while (R)-3HB-CoA was lower, suggesting an insufficient NADPH supply on acetate. However, the small amount of Ac-CA accumulated in the acetate condition suggests that it may not be easy to improve PHB production on acetate.

When fructose is utilized by *R. eutropha* H16, fructose can be catabolized through the ED pathway and the citric acid cycle [33] with enough energy, ATP and NADH, for cell growth. When prokaryotes use the ED pathway, only 1 ATP can be obtained, which is only half of that produced from prokaryotes that use the EMP pathway. This is reflected in the low AEC ratio. Based on the measured adenylate phosphates, the calculated AEC ratio also showed a lower value (about 0.6 on fructose) than the strains that metabolize glucose with the EMP pathway (Fig. 4(a)). In the case of *E. coli*, cells are known to grow only when the AEC ratio is over 0.8 [37]. However, *R. eutropha* H16 grows well with much lower AEC ratios on fructose, which can be the result of a lower metabolic burden for the ED pathway. A recent report suggested that the ED pathway requires substantially fewer enzymatic proteins than the EMP pathway and that the ED pathway yields less ATP than the EMP pathway [35]. This might explain why *R. eutropha* H16 can live with a much lower AEC ratio.

On the other hand, when an inefficient carbon source like acetate is catabolized, microbes activate the glyoxylate shunt pathway to reduce carbon loss via CO_2 [38,39]. Through the glyoxylate shunt pathway, one acetate molecule only produces 1 NADH and 1 $FADH_2$; thus, considerably low amounts of ATP can be generated via the electron transport system. Because the products of the glyoxylate pathway are converted to PEP for biosynthesis, 1.37 times more PEP was observed in the acetate condition compared to that on fructose. This is also explained by the very low AEC ratio on acetate (0.379) compared to that on fructose (0.645) (Fig. 2).

Compared with the results of extracellular and intracellular metabolite profiling, the two different carbon sources, fructose and acetate, had distinctive characteristics during PHB production. The production titer was higher on fructose while the specific production rate was higher on acetate. The accumulation of pre-cursor metabolites and low ATP availability were significant hurdles. Different but complementary approaches will provide an opportunity to use acetate as a carbon source for PHB production in *R. eutropha* H16.

ACKNOWLEDGEMENTS

This research was supported by a grant from the New & Renewable Energy Program of the Korea Institute of Energy Technology Evaluation and Planning (No. 20143030091040) and a grant from the National Research Foundation of Korea funded by the Korean Government (2012M1A2A2026560).

NOMENCLATURE

(R)-3HB-CoA : (R)-3-hydroxybutyryl-CoA
2PG : 2-phosphoglycerate
3PG : 3-phosphoglycerate
6PG : 6-phosphogluconate
AA-CoA : acetoacetyl-CoA
Ac-CoA : acetyl-CoA
Ac-Glu : acetyl-glutamic acid
ADP : adenosine di-phosphate
AEC : adenylate energy charge
aKG : alpha-ketoglutarate
Ala : alanine
AMP : adenosine mono-phosphate
Asn : asparagine
Asp : aspartic acid
ATP : adenosine tri-phosphate
CBB cycle : calvin-benson-bassham cycle
Cit : citrate
CRP : cAMP receptor protein
DHAP : dihydroxyacetone phosphate
E4P : erythrose 4-phosphate

F1,6bP : fructose 1,6-bisphosphate
F1P : fructose 1-phosphate
F6P : fructose-6-phosphate
Fum : fumarate
G1P : glucose 1-phosphate
G3P : glycerol 3-phosphate
G6P : glucose-6-phosphate
GAP : glyceraldehyde 3-phosphate
GC-EI-MS : gas chromatography with electron ionization coupled to mass spectrometer
Gln : glutamine
Glu : glutamate
Gly : glycine
iCit : iso-citrate
Ile : Isoleucine
LC/TOF/MS : liquid chromatography/time-of-flight mass spectrometer
Leu : leucine
Lys : lysine
Mal : malate
Met : methionine
Met : methionine
MS : mass spectrometry
OAA : oxaloacetate
P(3HB) : poly(3-hydroxybutyrate)
PBS buffer : phosphate-buffered saline buffer
PEP : phosphoenolpyruvate
PHA : polyhydroxyalknoates
Phe : phenylalanine
PRPP : phosphoribosylpyrophosphate
PYR : pyruvate
QTOF MS : quadrupole time-of-flight mass spectrometer
R5P : ribose-5-phoshpate
Ribu5P : ribulose 5-phosphate
S7P : sedoheptulose-7-phosphate
Ser : serine
Suc : succinate
SUC-CoA : succinyl-CoA
Thr : threonine
TSB medium : tryptic soy broth medium
Tyr : tyrosine
UPLC : ultra performance liquid chromatography
Val : valine
X5P : xylulose 5-phosphate

SUPPORTING INFORMATION

Additional information as noted in the text. This information is available via the Internet at http://www.springer.com/chemistry/journal/11814.

REFERENCES

1. S. Chanprateep, *J. Biosci. Bioeng.*, **110**, 621 (2010).
2. G.-Q. Chen, *Microbiol. Monograph.*, **14**, 17 (2010).
3. M. Koller, A. Salerno, A. Muhr, A. Reiterer and G. Braunegg, *Mater. Technol.*, **47**, 5 (2013).
4. T. Fukui, K. Chou, K. Harada, I. Orita, Y. Nakayama, T. Bamba, S. Nakamura and E. Fukusaki, *Metabolomics*, **10**, 190 (2014).
5. T. A. Leaf and F. Srienc, *Biotechnol. Bioeng.*, **57**, 557 (1998).
6. B. H. A. Rehm, *Biochem. J.*, **376**, 15 (2003).
7. C. Pena, T. Castillo, A. Garcia, M. Millan and D. Segura, *Microb. Biotechnol.*, **7**, 278 (2014).
8. D. Segura and G. Espin, *Appl. Microbiol. Biotechnol.*, **65**, 414 (2004).
9. R. Noguez, D. Segura, S. Moreno, A. Hernandez, K. Juarez and G. Espin, *J. Mol. Microbiol. Biotechnol.*, **15**, 244 (2008).
10. C. Pena, S. Lopez, A. Garcia, G. Espin, A. Romo-Uribe and D. Segura, *Ann. Microbiol.*, **64**, 39 (2014).
11. M. Akiyama, T. Tsuge and Y. Doi, *Polym. Degrad. Stab.*, **80**, 183 (2003).
12. C. F. Budde, S. L. Riedel, F. Hubner, S. Risch, M. K. Popovic, C. Rha and A. J. Sinskey, *Appl. Microbiol. Biotechnol.*, **89**, 1611 (2011).
13. S. L. Riedel, J. Bader, C. J. Brigham, C. F. Budde, Z. a. M. Yusof, C. Rha and A. J. Sinskey, *Biotechnol. Bioeng.*, **109**, 74 (2012).
14. O. Fiehn, *Plant Mol. Biol.*, **48**, 155 (2002).
15. M. R. Mashego, K. Rumbold, M. De Mey, E. Vandamme, W. Soetaert and J. J. Heijnen, *Biotechnol. Lett.*, **29**, 1 (2007).
16. D. Vuckovic, *Anal. Bioanal. Chem.*, **403**, 1523 (2012).
17. S. Kim, D. Y. Lee, G. Wohlgemuth, H. S. Park, O. Fiehn and K. H. Kim, *Anal. Chem.*, **85**, 2169 (2013).
18. X. Y. Wang, F. X. Yang, Y. S. Zhang, G. W. Xu, Y. Liu, J. Tian and P. Gao, *Electrophoresis*, **36**, 2140 (2015).
19. H. M. Lee, B. Y. Jeon and M. K. Oh, *Biotechnol. Bioproc. Eng.*, **21**(3), 402 (2016).
20. J. M. Buescher, S. Moco, U. Sauer and N. Zamboni, *Anal. Chem.*, **82**, 4403 (2010).
21. M. Friedman, *J. Agric. Food Chem.*, **52**, 385 (2004).
22. G. D. Saratale and M. K. Oh, *Int. J. Biol. Macromol.*, **80**, 627 (2015).
23. B. Gonzalez, J. Francois and M. Renaud, *Yeast*, **13**, 1347 (1997).
24. N. B. S. Jensen, K. V. Jokumsen and J. Villadsen, *Biotechnol. Bioeng.*, **63**, 356 (1999).
25. R. P. Maharjan and T. Ferenci, *Anal. Biochem.*, **313**, 145 (2003).
26. B. Álvarez-Sánchez, F. Priego-Capote and M. D. Luque de Castro, *Trends Analyt. Chem.*, **29**, 120 (2010).
27. C. L. Winder, W. B. Dunn, S. Schuler, D. Broadhurst, R. Jarvis, G. M. Stephens and R. Goodacre, *Anal. Chem.*, **80**, 2939 (2008).
28. R. D. Douma, L. P. De Jonge, C. T. H. Jonker, R. M. Seifar, J. J. Heijnen and W. M. Van Gulik, *Biotechnol. Bioengin.*, **107**, 105 (2010).
29. L. P. De Jonge, R. D. Douma, J. J. Heijnen and W. M. Van Gulik, *Metabolomics*, **8**, 727 (2012).
30. W. M. Van Gulik, *Curr. Opin. Biotechnol.*, **21**, 27 (2010).
31. C. Wittmann, J. O. Kromer, P. Kiefer, T. Binz and E. Heinzle, *Anal. Biochem.*, **327**, 135 (2004).
32. G. D. Tredwell, B. Edwards-Jones, D. J. Leak and J. G. Bundy, *Plos One*, **6** (2011).
33. A. Pohlmann, W. F. Fricke, F. Reinecke, B. Kusian, H. Liesegang, R. Cramm, T. Eitinger, C. Ewering, M. Potter, E. Schwartz, A. Strittmatter, I. Voss, G. Gottschalk, A. Steinbuchel, B. Friedrich and B. Bowien, *Nat. Biotechnol.*, **25**, 478 (2007).
34. Y. Jian and Y. Si, *Biotechnol. Prog.*, **20**, 1015 (2004).
35. G. Gottschalk, H. G. Schlegel and U. Eberhardt, *Arch. Microbiol.*, **48**, 95 (1964).

36. R. Gerstmeir, V. F. Wendisch, S. Schnicke, H. Ruan, M. Farwick, D. Reinscheid and B. J. Eikmanns, *J. Biotechnol.*, **104**, 99 (2003).
37. M. K. Oh, L. Rohlin, K. C. Kao and J. C. Liao, *J. Biol. Chem.*, **277**, 13175 (2002).
38. A. G. Chapman, L. Fall and D. E. Atkinson, *J. Bacteriol.*, **108**, 1072 (1971).
39. Z.-X. Wang, C. O. Brämer and A. Steinbüchel, *FEMS Microbiol. Lett.*, **228**, 63 (2003).
40. H. L. Kornberg and H. A. Krebs, *Nature*, **179**, 988 (1957).

Supporting Information

Comparison of metabolite profiling of *Ralstonia eutropha* H16 *phaBCA* mutants grown on different carbon sources

Dae-Kyun Im[*,‡] Seok Hun Yun[,***,‡], Joon-Young Jung[**], Jinwon Lee[***,†], and Min-Kyu Oh[*,†]**

*Department of Chemical and Biological Engineering, Korea University, Seoul 02841, Korea
**CJ Research Institute of Biotechnology, Suwon 16495, Korea
***Department of Chemical and Biomolecular Engineering, Sogang University, Seoul 04107, Korea
(*Received 24 October 2016 • accepted 20 November 2016*)

Additional Supporting Information may be found in the online version of this article:

Table S1. Chromatographic gradient used to separate metabolites by liquid chromatography with mobile phases

UPLC condition (intracellular metabolites analysis)						
Phase A	10 mM tributylamine, 15 mM acetic acid in distilled water					
Phase B	100% methanol					
Time (min)	%A					%B
0	98					2
5	98					2
30	20					80
32	20					80
32.1	98					2
36	98					2
TAA condition (extracellular amino acids analysis)						
Phase A	pH buffer and stabilizing solutions					
Phase B	ninhydrin solution					
Time (min)	%A (separation column)					%B (reaction column)
	B1	B2	B3	B4	RG	
0	100					100
3						
3.1		100				
7						
7.1			100			
14.8						
14.9				100		
29						
29.1					100	
32						

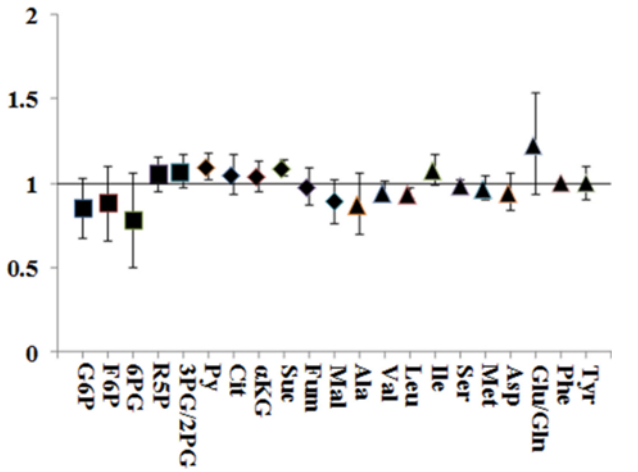

Fig. S1. Correlation values of measured metabolite level using GC-EI-MS and LC-TOF-MS. These values were calculated using followed equation ($Metabolite_{GC\text{-}EI\text{-}MS}$/$Metabolite_{LC\text{-}TOF\text{-}MS}$), Sugar phosphate (■) showed relatively high deviation than organic acids (◆) and amino acids (▲).

Table S2. Total amino acids analysis of WT strain during cultivation at two points (#1: start, #2: metabolite profiling sampling time)

C-source	Acetate				‘Fructose			
Sampling time	#1		#2		#1		#2	
Unit (mg/L)	Average	STD	Average	STD	Average	STD	Average	STD
Asp	1.730	0.067	0.984	0.087	1.793	0.096	2.861	0.349
Thr	1.602	0.058	0.000	0.000	1.636	0.037	1.889	0.032
Ser	1.565	0.056	3.551	0.476	1.586	0.040	2.483	0.210
Glu	4.511	0.046	37.279	2.849	4.302	0.101	61.218	2.315
Gly	0.493	0.020	1.615	0.297	0.479	0.020	0.000	0.000
Ala	2.026	0.067	4.891	0.273	1.925	0.065	3.136	0.230
Cys	0.000	0.000	0.000	0.000	0.000	0.000	0.000	0.000
Val	3.899	0.097	2.565	0.076	3.863	0.110	2.516	0.107
Met	2.305	0.144	1.416	0.386	2.386	0.201	1.483	0.335
Ile	1.527	0.118	0.000	0.000	1.637	0.063	0.000	0.000
Leu	8.338	0.205	0.768	0.071	8.560	0.094	0.000	0.000
Tyr	1.535	0.134	2.685	0.126	1.401	0.080	3.243	0.522
Phe	5.636	0.091	3.502	0.395	5.818	0.414	3.004	0.313
Lys	4.504	0.050	0.000	0.000	4.663	0.049	0.808	0.090
His	0.000	0.000	0.000	0.000	0.000	0.000	0.000	0.000
Arg	3.447	0.118	4.444	0.455	3.477	0.050	0.000	0.000

Analysis was performed, biological triplicates and technical duplicates (n=6)